Available online at www.sciencedirect.com
SCIENCE DIRECT®
Journal of Chromatography A, 1012 (2003) 1–10
JOURNAL OF CHROMATOGRAPHY A
www.elsevier.com/locate/chroma

Modeling of the whole expanded-bed protein adsorption process with yeast cell suspensions as feedstock

Wei-Dong Chen, Xiao-Yan Dong, Yan Sun*

Department of Biochemical Engineering, School of Chemical Engineering and Technology, Tianjin University, Tianjin 300072, China

Received 3 April 2003; received in revised form 1 July 2003; accepted 2 July 2003

Abstract

Expanded bed adsorption of bovine serum albumin (BSA) directly from a feedstock containing whole yeast cells has been investigated with an anion-exchanger DEAE Spherodex M. In the presence of 6% (w/w) yeast cells, the axial liquid-phase dispersion coefficient was found in the order of 10^{-6} m^2/s, which felled into the common range of $1.0\cdot10^{-6}$–$1.0\cdot10^{-5}$ m^2/s observed previously without the use of cell suspensions as mobile phase. We found that the static and dynamic binding capacity of BSA decreased with increasing the yeast cell concentration due to the competitive adsorption of cells onto the outer surface of the anion-exchanger. However, because of the small size of the adsorbent, the large pore diffusivity of protein and the favorable column efficiency (low axial dispersion coefficient), the dynamic binding capacity of BSA in the presence of 6% (w/w) cells in the expanded bed reached 86% that of the equilibrium adsorption density. Then, the whole expanded bed adsorption process of BSA in the presence of cells, including feedstock loading, washing and elution steps, was predicted using a mathematical model with parameters all determined independently. In the elution stage, the steric mass-action adsorption isotherm with salt concentration as one of the model parameters was used to predict the step-gradient elution process with salt concentration increases. Computer simulations showed that the model was in good agreement with the experimental results for the whole operation process.

Keywords: Expanded bed chromatography; Yeast; Mathematical modelling; Albumin; Proteins

1. Introduction

Expanded bed is a low back-mixing liquid fluidized bed obtained by the special design of the column, liquid distributor and solid matrix with a defined size and/or density distribution. As an innovative chromatography mode, expanded bed adsorption (EBA) has great advantages over the conventional packed-bed chromatography [1,2]. EBA is a single-pass unit operation in which proteins are recovered and concentrated from crude feedstock and transferred to a process for further chromatographic purification, without the need for feedstock clarification [3]. Over the past decade, a number of successful applications in the expanded bed with variety of biological systems, such as whole yeast, mammalian cells and their homogenates and so on, have been reported in literature [4–8]. The results show that any expanded bed adsorbent selected must be such

*Corresponding author. Tel.: +86-22-2740-4981; fax: +86-22-2740-6590.
E-mail address: ysun@tju.edu.cn (Y. Sun).

0021-9673/03/$ – see front matter
doi:10.1016/S0021-9673(03)01182-8

that it is resistant to fouling and degradation when operating in crude process liquids [9,10].

We have demonstrated that it is possible to establish a stable expanded bed using DEAE Spherodex M, which has very high protein adsorption capacity [11]. Experimental data of residence time distributions has shown that liquid flow through the bed is close to plug flow. Moreover, it is found that the adsorption efficiency in the expanded bed of DEAE Spherodex M is less affected by the liquid flow velocity and viscosity. In order to check the potentials of the exchanger in the direct extraction of proteins from fermentation broths, it is necessary to investigate the EBA performance of DEAE Spherodex M in the presence of cells.

Thus, on the basis of our previous work studying the hydrodynamics and protein adsorption properties in the expanded bed of anion-exchange, DEAE Spherodex M [11], the influence of whole cells on the static and dynamic protein binding capacity of the exchanger are investigated in the present work. A suspension of bovine serum albumin (BSA) and 6% (w/w) yeast cells was used for the EBA experiments. A mathematical theoretical model for the whole expanded bed adsorption process, including feedstock loading, washing and elution steps, was developed on the basis of previous work [3,11,12]. In the feed loading and washing steps, the Langmuir equation was employed to describe the adsorption isotherm. In the elution step, however, the steric mass-action formulism [13,14] with salt concentration as a variable was used as the adsorption isotherm to effectively depict the salt effect on the elution process. The whole EBA process has been predicted using the model with unadjustable model parameters and compared with the experimental results.

2. Materials and methods

2.1. Materials

BSA (fraction V, minimum 96%) was purchased from Sigma (St. Louis, MO, USA). Anion-exchanger, DEAE Spherodex M (size range 61–120 μm, volume-weighted mean size 88 μm), was obtained from BioSepra (Cergy-Saint-Christophe, France). Baker's yeast (*Saccharomyces cerevisiae*) was obtained in the form of pressed blocks from Hebei Mali Foods (Changli, China). All other reagents are of analytical grade from local sources.

2.2. Batch adsorption experiments

Suspensions of washed yeast cells in 0.01 mol/l phosphate buffer pH 7.6 were used in the present work. Adsorption equilibrium and kinetic experiments of BSA on the anion-exchanger were performed using the stirred batch adsorption method in 0.01 mol/l phosphate buffer (pH 7.6) containing up to 6% (w/w) cells at 25 °C. Here, cell amount is expressed as wet weight.

In adsorption equilibrium experiments, a known amount of the anion-exchanger pre-equilibrated in the buffer was added to each of the flasks containing known volume of buffered protein solution with different concentrations (0.1–2.6 mg/ml) and yeast cells. The flasks were shaken for 10 h in a shaking water bath at 25 °C, which had been confirmed to be sufficient to reach adsorption equilibrium. The suspension was then centrifuged at 4000 rpm for 10 min (to settle the yeast cells and/or adsorbent particles) and the equilibrium protein concentration in the supernatant was determined with a Model 9100 UV–Vis spectrophotometer at 280 nm. The amount of protein adsorbed to the DEAE Spherodex M was calculated by mass balance. Control experiments were also performed without adding BSA to the adsorption system. In the control experiments, the ion-exchange particles were allowed to gravity-settle and the equilibrium cell concentration in the supernatant was determined spectrophotometrically at 600 nm, while the equilibrium protein concentration was measured at 280 nm after centrifuging at 4000 rpm for 10 min to remove the cells.

The pore diffusivity of BSA was determined in the phosphate buffer with a constant yeast cell concentration using the stirred batch adsorption method as stated previously [15].

2.3. Expanded bed experiments

Expanded a glass column (70 cm×9.5 mm I. D.) was used for all expanded bed experiments. A stainless steel mesh of 54 μm pores was installed in

the column bottom as the flow distributor and a top adapter was positioned 1.0±0.2 cm above the bed surface in each expanded bed experiment. The experimental protocols were the same as those described previously [16]. The phosphate buffer containing 6% yeast cells was used as the liquid-phase for the expanded bed experiments. Liquid-phase dispersion behavior in the expanded bed was determined by the residence time distribution (RTD) method as stated previously [11].

The loading, washing and elution behaviors of yeast cells and BSA in the expanded bed of the anion-exchanger were investigated. In order to prevent the trapping of particulate materials in the bed, the elution stage was also carried out in the expanded bed configuration. All experiments were carried out in the presence of 6% cells at 25 °C with a settled bed height of 6.9±0.2 cm and the feedstock BSA concentration was 2.0 mg/ml. The BSA loading and elution steps were carried out at a bed expansion degree of 2.5, while the washing stage was performed at a bed expansion degree of 3.5. Before applying feedstock, the bed was allowed to expand to a stable bed expansion degree of 2.5 for more than 30 min with the phosphate buffer, and the flow hydrodynamics of the beds was determined at first. Then, the feedstock was loaded onto the column. The liquid flow velocity was increased gradually during the adsorption process to keep the constant bed expansion degree. The average liquid velocity was calculated from the ratio of total feed volume supplied to column to the operation time in the loading process. When measurement of the breakthrough curve was completed, the system was switched to the phosphate buffer to wash out the excess protein and cells from the column until the effluent absorbance reached a steady value. Then, the elution was performed using 0.01 mol/l phosphate buffer pH 7.6 containing 0.1 and/or 0.2 mol/l NaCl. The dynamic binding capacity (DBC) was determined as stated previously [16]. During the whole operation process, the outlet stream from the bed was collected every 5–10 ml. The yeast cell concentration in the collected pool was determined spectrophotometrically at 600 nm. The protein concentration was measured at 280 nm after centrifugation for 10 min at 4000 rpm. Control experiments were also performed without adding BSA in the feedstock. The experimental procedure in the control experiments was the same as described above. All expanded bed experiments were done on the Äkta explorer 100 (Amersham Pharmacia Biotech, Uppsala, Sweden).

2.4. Analysis and measurements

The particle size distribution of DEAE Spherodex M was measured with a Malvern Mastersizer 2000 particle analyzer (Malvern Instruments, Worcestershire, UK). The wet density of the resin was measured by a pycnometer at 25 °C. The effective intraparticle porosity of the DEAE Spherodex M for protein was determined using a batch diffusion technique [17]. The morphology of DEAE Spherodex M was observed with a model XS-18 optical microscope (Jiangnan Scientific Instruments China), and the image was recorded with a Model YT-310B CCD (charge coupled device) camera.

3. Expanded-bed adsorption model

The expanded bed adsorption model is constructed on the basis of the following assumptions:

(1) The adsorbent particles are spherical, with uniform size and density, and the functional groups of the ion-exchanger are evenly distributed throughout the interior surface of the particles.

(2) Protein concentration in the adsorbent pore is in local equilibrium with its concentration adsorbed on the inner surface of the pore wall. In the adsorption and washing stages, this equilibrium is represented by the Langmuir equation:

$$q = \frac{q_m C}{K_d + C} \tag{1}$$

In the elution step, however, this equilibrium is represented by the SMA formulism [13,14] with salt concentration as a variable:

$$C = \left(\frac{q}{K_a}\right)\left(\frac{nC_s}{A - (\nu + n\sigma_a)\, q}\right)^{\frac{\nu}{n}} \tag{2}$$

(3) The rate of protein adsorption to the adsorbent is controlled by intraparticle diffusion and the external liquid-film mass transfer resistances.

(4) The hydrodynamic behavior of the solid and

liquid phases can be described by the axial dispersion model [18]. For the liquid phase, the model is written as:

$$\varepsilon_L \cdot \frac{\partial C}{\partial t} = D_{ax,L}\varepsilon_L \cdot \frac{\partial^2 C}{\partial Z^2} - u \cdot \frac{\partial C}{\partial Z} - \frac{3k_f\varepsilon_s(C - C_{p,r=R})}{R} \quad (3)$$

The initial and boundary conditions for the loading step are:

$$\text{IC:} \quad t = 0, \quad 0 \le Z \le H, \quad C(Z,0) = 0 \quad (3a)$$

$$\text{BC1:} \quad t > 0, \quad Z = 0, \quad C = C_0 + \frac{D_{ax,L}\varepsilon_L}{u} \cdot \frac{\partial C}{\partial Z} \quad (3b)$$

$$\text{BC2:} \quad t > 0, \quad Z = H, \quad \frac{\partial C}{\partial Z} = 0 \quad (3c)$$

For the solid-phase, there is no convective flow. Hence, the axial dispersion model for the solid-phase is expressed as:

$$\varepsilon_s \cdot \frac{\partial q'}{\partial t} = D_{ax,s} \cdot \frac{\partial^2 q'}{\partial Z^2} + \frac{3k_f\varepsilon_s(C - C_{p,r=R})}{R} \quad (4)$$

The values for the solid dispersion coefficient $D_{ax,s}$ and the film mass transfer coefficient k_f are, respectively, calculated by [18,19]:

$$D_{ax,s} = 0.04u^{1.8}\ (m^2/s) \quad (5)$$

$$k_f = \frac{D_\infty}{d_p} \cdot \left[2 + 1.5(1 - \varepsilon_L)\, R_{\varepsilon,p}^{\frac{1}{2}} S_c^{\frac{1}{3}} \right] \quad (6)$$

Eq. (4) is solved using the following initial and boundary conditions for the loading step:

$$\text{IC:} \quad t = 0, \quad 0 \le Z \le H, \quad q'(Z,0) = 0 \quad (4a)$$

$$\text{BC1:} \quad t > 0, \quad Z = 0, \quad \frac{\partial q'}{\partial Z} = 0 \quad (4b)$$

$$\text{BC2:} \quad t > 0, \quad Z = H, \quad \frac{\partial q'}{\partial Z} = 0 \quad (4c)$$

Our previous work has shown that protein transport to the anion-exchanger could be well described by the pore diffusion model (PDM) [17]. The PDM is described by:

$$\varepsilon_p \cdot \frac{\partial C_p}{\partial t} = \varepsilon_p D_p \frac{1}{r^2} \cdot \frac{\partial}{\partial r}\left(r^2 \cdot \frac{\partial C_p}{\partial r} \right) - \frac{\partial q}{\partial t} \quad (7)$$

The initial and boundary conditions of this equation for the loading step are:

$$\text{IC:} \quad t = 0, \quad 0 \le Z \le H, \quad C_p = 0, \quad q = 0 \quad (7a)$$

$$\text{BC1:} \quad t > 0, \quad r = 0, \quad \frac{\partial C_p}{\partial r} = 0, \quad \frac{\partial q}{\partial r} = 0 \quad (7b)$$

$$\text{BC2:} \quad t > 0, \quad r = R, \quad \frac{\partial C_{p,r=R}}{\partial r} = \frac{R}{3\varepsilon_p D_p} \cdot \frac{\partial q'}{\partial t} \quad (7c)$$

The above equations (Eqs. (3)–(7)) are also used for expressing the washing and elution steps ($C_0 = 0$), except that the three initial conditions described by Eqs. (3a), (4a) and (7a) are set as those at the end of the loading and washing steps, respectively.

Along with the initial and boundary conditions, the above model equations for EBA process are discretized by the Hermite finite element method with 15 evenly spaced finite element points along the column length, and the governing equation for the intraparticle mass transfer (Eq. (7)) is solved by the orthogonal collocation method [20]. The number of collocation points in the radial direction of the adsorbent is set at five. The number of finite element and collocation points is found to give sufficient accuracy.

4. Results and discussion

4.1. Effect of cells on protein adsorption

An optical microscopic observation has shown that yeast cells were adsorbed on the surface of DEAE Spherodex M in phosphate buffer pH 7.6 (data not shown). Therefore, in order for the study of the influence of whole cells on the static and dynamic protein binding capacity of the exchanger, the cell adsorption behavior in the absence of BSA was first investigated by batch and expanded-bed adsorption experiments. Batch adsorption results showed that the adsorption equilibrium of yeast cells to the anion-exchanger could be approximately described by a linear relationship (data not shown). Though cells are

basically adsorbed on the outer surface of the anion-exchanger, the value of cell equilibrium adsorption density at a liquid-phase yeast cell concentration of 6% reached as high as 350 mg/ml. This value was much higher than the adsorption capacity of BSA in the absence of cells (169.5 mg/ml) (Table 1). It is considered due to the large dimension of yeast cells.

The results of EBA experiments with 6% yeast cell suspension in the absence of BSA showed that the adsorbed cells could be efficiently washed out by increasing the volume of the washing buffer (0.01 mol/l phosphate buffer pH 7.6) (data shown below). This means that the binding strength between the cells and the anion-exchanger was small. In addition, cell adsorption experiments confirmed that there was negligible protein release from the cells under the conditions investigated. This is in agreement with that reported by Chase and Draeger [9,10].

The effect of yeast cells on BSA adsorption equilibrium to the ion-exchanger was investigated by the measurement of the protein adsorption isotherms at different cell concentrations. Fig. 1 shows the results. In the presence of cells, the adsorption equilibrium data of BSA to the anion-exchanger can also be well fitted to the Langmuir equation (Eq. (1)). The Langmuir equation coefficients (K_d and q_m) for BSA obtained by nonlinear least-squares regression are summarized in Table 1. It can be found from Table 1 that the value of q_m decreased by 17%, while the value of K_d increased by nearly one order of magnitude with increasing cell concentration from 0 to 6%. Similar observations on BSA adsorption to the anion-exchanger Q Sepharose Fast Flow have been reported in the presence of *Saccharomyces cerevisiae* or *Alcaligenes eutrophus* cells [9,21]. The adsorption of cells on anion-exchanger is considered due to the negatively charged cell surface at a neutral buffer [9]. Cells are adsorbed onto the anion-exchanger surface by competitive adsorption with proteins on the adsorption sites. In addition, the absorption of cells can block the micropores of the adsorbent, preventing protein from accessing to the interior binding sites. Because the adsorption density of yeast cells increases linearly with increasing cell concentration (see above), protein adsorption capacity decreases with increasing cell concentration (Fig. 1 and Table 1).

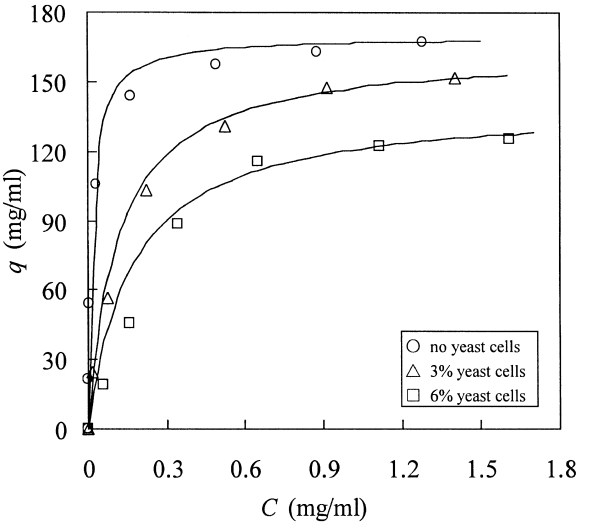

Fig. 1. Effects of yeast cell concentration on the adsorption isotherms of BSA to DEAE Spherodex M. Solid lines are calculated from the Langmuir equation.

Table 1
Static and dynamic adsorption results of BSA to DEAE Spherodex M[a]

Run no.	Cell concentration (% w/w)	q_m (mg/ml)	K_d (mg/ml)	u (cm/h)	DBC[b] (mg/ml)	DBC/EAD[c] (−)
1	0	169.5	0.017	126[d]	146[d]	0.87[d]
2	3	163.9	0.115	–	–	–
3	6	140.8	0.169	42.1	111.1	0.86

[a] Experimental conditions for EBA were $H_0 = 6.9 \pm 0.2$ cm, $H/H_0 = 2.5$, $C_{0,BSA} = 2.0$ mg/ml.
[b] DBC stands for dynamic binding capacity at 5% breakthrough.
[c] EAD stands for equilibrium adsorption density at $C = 2.0$ mg/ml, calculated from the Langmuir equation using the q_m and K_d values (run no. 1 or 3) listed in this table.
[d] Data from Ref. [11].

4.2. EBA process

We found that the bed expansion characteristics also obeyed the Richardson–Zaki equation [22] with yeast cell suspension as the liquid phase (data not shown), and the Richardson–Zaki coefficients increased with either increasing the viscosity of the fluidizing liquid or the settled bed height. Moreover, the axial liquid-phase dispersion coefficients in the expanded bed with cell suspensions as the liquid phase increased with either increasing liquid flowrate or liquid viscosity (data not shown). These results were all similar to those reported previously in the absence of cells [11,12,23,24]. The axial liquid-phase dispersion coefficient was measured in the order of 10^{-6} m^2/s in the presence of cells (Table 2), within the common range of $1.0\cdot10^{-6}$–$1.0\cdot10^{-5}$ m^2/s observed previously [25,26]. The results suggest that DEAE Spherodex M is suitable for efficient expanded bed operation in the presence of whole cells.

The EBA process of BSA in the adsorption (feed loading), washing and elution stages in the presence of 6% cells was then investigated. In the elution step, we tested two elution protocols. The first one was a two-stage stepwise elution protocol (experiment 1). That is, 0.01 mol/l phosphate buffer pH 7.6 with 0.1 mol/l NaCl was used as the first elution buffer and the phosphate buffer with 0.2 mol/l NaCl as the second elution buffer (Fig. 2). The second one was a one-stage elution strategy (experiment 2); the phosphate buffer pH 7.6 with 0.2 mol/l NaCl was used as elution buffer (Fig. 3). The dynamic binding capacity (DBC) of BSA at 5% breakthrough was estimated as described earlier [11] and results are listed in Table 1. In the absence of cells, the ratio of the DBC to the equilibrium adsorption density (EAD) was as high as 0.87, and it was equal to 0.86 in the presence of 6% yeast cells. These two values are nearly the same, indicating the high efficiency of the EBA system with cell suspensions as feedstock. The ratio (0.86) is even higher than that found for BSA adsorption in the expanded bed of Streamline DEAE in the absence of cells (0.60–0.68) [27]. The high dynamic binding efficiency of DEAE Spherodex M is considered due to the following reasons. (1) The mean size of DEAE Spherodex M is over twofold smaller than the Streamline particles. In addition, the pore diffusivity of proteins in DEAE Spherodex M is very large [17]. For example, the pore diffusivity of BSA was estimated as high as 2.19×10^{-11} m^2/s

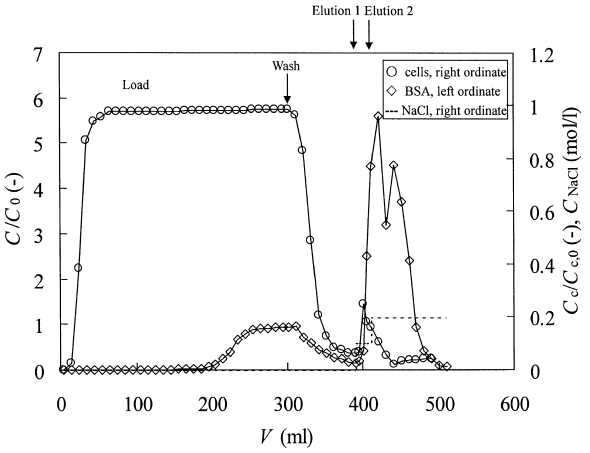

Fig. 2. Chromatographic profile of BSA and cells in the EBA process with 6% yeast cells as feedstock (exp. 1). Broken lines denote the salt concentrations of the elution buffers, the first elution buffer was 0.01 mol/l phosphate buffer with 0.1 mol/l NaCl, and the second elution buffer was the phosphate buffer with 0.2 mol/l NaCl. $H_0=6.9\pm0.2$ cm, $C_{0,BSA}=2.0$ mg/ml.

Table 2
Physical properties of the liquid-phases and the EBA model parameters for the loading (6% yeast cells), washing and elution steps

Stage	μ (10^{-3} Pa·s)	ρ (10^3 kg/m^3)	u (cm/h)	H/H_0	$D_{ax,L}$ [a] (10^{-6} m^2/s)	D_p [b] (10^{-11} m^2/s)	k_f (10^{-6} m/s)
Load (exp. 1)	3.0	1.01	42.1	2.5	4.6	2.19	2.60
Load (exp. 2)	3.0	1.01	41.0	2.5	4.6	2.19	2.59
Wash	1.0	1.0	187.2	3.5	7.2	5.12	3.27
Elution	1.0	1.0	90	2.5	3.52	5.12	3.31

[a] Axial dispersion coefficient determined by residence time distribution method [11].
[b] Pore diffusivity of BSA determined by dynamic batch adsorption method [15].

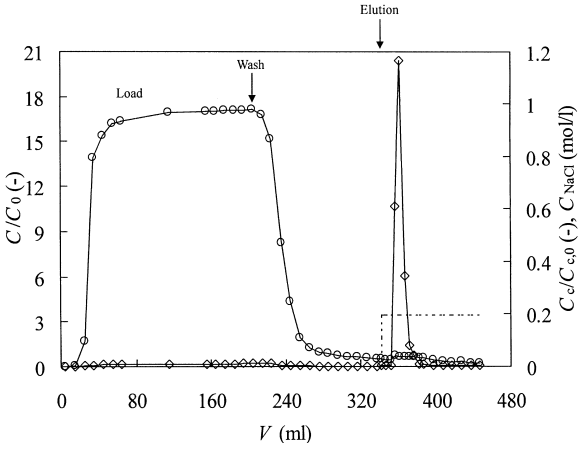

Fig. 3. Chromatographic profile of BSA and cells in the EBA process with 6% yeast cells as feedstock (exp. 2). Broken line denotes the salt concentration of elution buffer (0.01 mol/l phosphate buffer with 0.2 mol/l NaCl). Symbols and columns are the same as in Fig. 2.

(Table 2) even in the presence of 6% cells. (2) Because of the small size of DEAE Spherodex M, its expanded bed at expansion degrees of 2.5 is operated at lower flow velocities than the expanded bed of Streamline. Longer residence time of protein in expanded bed may benefit in reaching higher DBC [3].

Table 3 summarizes that the yields and the concentration factors (CF) of BSA, and the cell removal factor (CRF) obtained in the two EBA experiments. In experiment 1, the protein yield and CF value were relative low, namely 74.7% and 3.1, respectively. It is due to the 100% breakthrough of BSA in the loading stage and the two-stage stepwise elution protocol adopted (Fig. 2). In experiment 2, the protein yield and CF values reached as large as 96 and 11.6%, respectively, because the loading was stopped at 5% BSA breakthrough and one stage elution strategy was adopted (Fig. 3). In Table 3, the CRF was defined by the following equation:

$$\mathrm{CRF} = \left(1 - \frac{V_e \cdot C_{c,e}}{V_f \cdot C_{c,0}}\right) \cdot 100\% \quad (8)$$

where V_f and V_e are the volumes of loaded feedstock and collected elution pool, respectively, and $C_{c,0}$ and $C_{c,e}$ are the cell concentrations in the feedstock and the collected elution pool, respectively. It can be seen that the values of CRF reached about 98% in both experiments. The results further confirmed that the cells adsorbed on the adsorbent could be efficiently washed out during washing process.

4.3. Modeling of the whole EBA process

To predict the chromatographic behavior of BSA in the EBA process, the parameters in the EBA model described above were determined by independent experiments or from correlations reported in literature. As elsewhere described [11], DEAE Spherodex M has an ion-exchange capacity (A) of 53.0 mM and a wet density of 1.27 g/ml. The statistics of the particle size distribution indicate that 80% by volume are in the range of 61–120 μm, and a volume-weighted mean diameter d_p is 88 μm. The ε_p value of DEAE Spherodex M for BSA was measured to be 0.616±0.023. The values of D_p and $D_{ax,L}$ measured by our experiments and the value of k_f calculated from Eq. (6) are listed in Table 2. These data with Langmuir equation coefficients for BSA (Table 4) are used in the model calculation for loading and washing stages.

To model the salt effect in the elution step, the

Table 3
Purification of BSA in the presence of 6% yeast cells using the expanded bed of DEAE Spherodex M

Exp. no.	Cell or BSA	Loaded (mg)	Eluted (mg)	CF[a]	BSA yield (%)	CRF[b] (%)
1	Cell	18 120	465.7	–	–	97.4
	BSA	604	451.2	3.1	74.7	–
2	Cell	12 600	172.9	–	–	98.6
	BSA	420	403.7	11.6	96.1	–

[a] CF stands for concentration factor of BSA.
[b] CRF refers to as cell removal factor.

Table 4
Adsorption equilibrium parameters used for the loading (6% yeast cells), washing and elution steps of the EBA process ($A=53.0$ mM, $n=1$)

Stage	q_m (mg/ml)	K_d (mg/ml)	K_a	ν	σ_a
Load (exp. 1)	140.8	0.169	–	–	–
Load (exp. 2)	140.8	0.169	–	–	–
Wash	169.5	0.017	–	–	–
Elution	–	–	1253	3.7	10.1

adsorption equilibrium in elution stage is described by the SMA model (Eq. (2)) where salt concentration is incorporated as a model parameter [13,14,28]. Fig. 4 shows the effect of NaCl concentration on BSA adsorption isotherm. Although the counterions consist of Cl^-, $H_2PO_4^-$, HPO_4^{2-} and PO_4^{3-} in the phosphate buffer containing NaCl, the phosphate concentration was much lower than Cl^-. So we take $n=1$ for the sake of simplicity. Using the experimental data shown in Fig. 4, the SMA model parameters are estimated by nonlinear least-square fitting, and listed in Table 4. It can be seen from Fig. 4 that the SMA model can well describe the effect of salt concentration on BSA adsorption equilibrium.

Thus, using the model parameters listed in Tables 2 and 4, the whole EBA process was simulated using the EBA model. Figs. 5 and 6 show the comparisons between the model simulations and the EBA profiles. As can be seen, the model prediction with the independently determined model parameters agreed well with the experimental results at protein breakthrough less than about 50% (see Fig. 5). In the later stage of breakthrough, however, the predicted curve was lower than the experimental data, which is opposite to the trend observed without adding cells [11]. The deviation of the model prediction at the

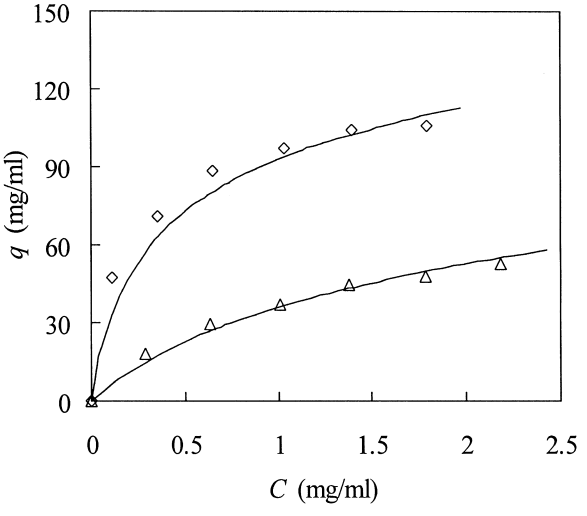

Fig. 4. Adsorption isotherm of BSA to DEAE Spherodex M in 0.01 mol/l phosphate buffer pH7.6 with different NaCl concentrations. Solid lines are calculated from the SMA model. The concentrations of salt counterions are (◇) 0.0671, and (△) 0.1171 mol/l.

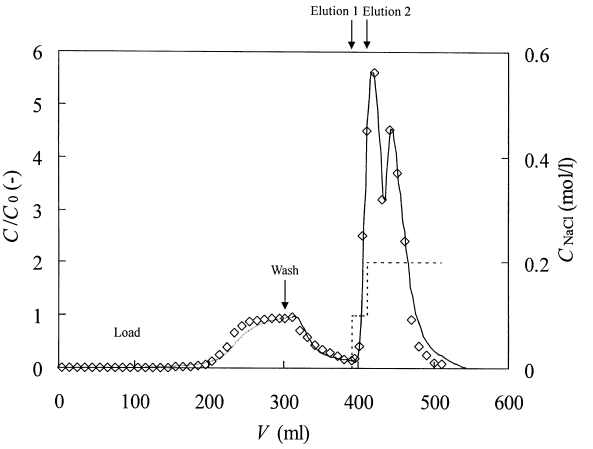

Fig. 5. Experimental and simulated chromatographic profiles of BSA in the EBA process with 6% yeast cells as feedstock (exp. 1). Solid line is calculated from the EBA model.

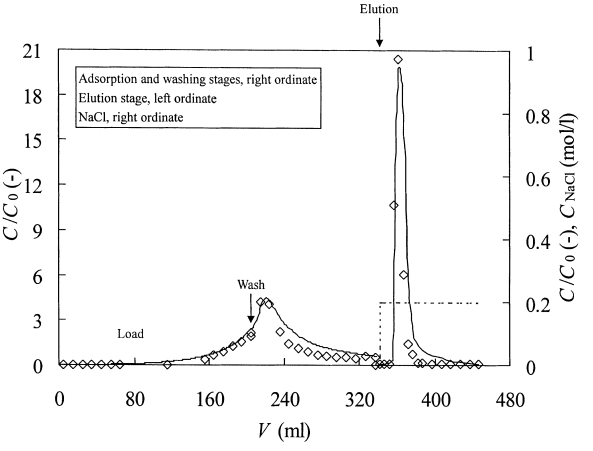

Fig. 6. Experimental and simulated chromatographic profiles of BSA in the EBA process with 6% yeast cells as feedstock (exp. 2). Solid line is calculated from the EBA model.

later stage of the breakthrough curve may be caused by the neglected protein released from the cells that would result in additional absorbance at 280 nm.

Figs. 5 and 6 show that the theoretical predictions with the SMA formulism agreed well with the experimental results at elution process except for slightly lower elution peak and longer tailing predictions. This indicates that the SMA formulism is a favorable isotherm to predict the step-gradient elution process.

In general, the mathematical model has proved to well describe the whole EBA process with cell suspensions as feedstock. The small deviations may be due to protein release from cells and the disregard of the solid-phase distribution in the expanded bed. It has been well know that solid-phase in expanded bed system has significant distributions of size and voidage along the column axis [29], so the assumption of even dispersion of the adsorbents in expanded bed may result in some model discrepancy. Wright and Glasser [3] reported that the effect of particle size on EBA was greater than the other parameters such as pore diffusivity and axial dispersion coefficients. Therefore, the EBA model might to be further improved by taking into account the distributions of the particle size and concentration.

Moreover, it should be noted that the feedstock used in this work was rather simplistic than a practical feedstock such as cell disruptate or fermentation broth, and behaves more like a model feedstock than the type that might be encountered during industrial operations. Thus, in further work using an industrial feedstock, the information for the adsorbent to foul and subsequently destabilize the expanded bed may well be much more pronounced.

5. Conclusions

In this article, the expanded bed of DEAE Spherodex M for the direct adsorption of protein from feedstocks containing yeast cells has been studied. The anion-exchanger showed high adsorption of the yeast cells, leading the decrease of BSA adsorption. In spite of this, the dynamic capacity remained very high, reaching 86% that of its static binding density. This is due to the favorable properties of the anion-exchanger in bed expansion, axial mixing characteristics and protein dynamic adsorption. Moreover, the yeast cells adsorbed on the adsorbent could be mostly washed out during the washing process, and a cell removal factor of 98% was achieved in the eluted protein pool. Furthermore, the whole EBA process for BSA recovery from yeast cell suspensions has been well described by the EBA model. SMA formulism was found to be favorable to predict the step-gradient elution process. It is considered that the model might be further improved by taking into account the distributions of adsorbent size and concentrations along the column.

6. Nomenclature

A	ion-exchange capacity (monovalent salt counterions), mM
C	protein concentration in bulk phase, mg/ml (mM in Eq. (2))
C_0	protein concentration in feedstock, mg/ml
C_p	protein concentration in pore, mg/ml
C_s	salt concentration in bulk phase, mM
d_p	mean particle diameter, m
$D_{ax,L}$	axial liquid-phase dispersion coefficient, m^2/s
$D_{ax,s}$	axial solid-phase dispersion coefficient, m^2/s
D_p	pore diffusivity in pore diffusion model, m^2/s
D_∞	diffusivity of protein in infinitely dilute solution, m^2/s
H	expanded bed height, cm
H_0	settled bed height, cm
k_f	liquid-film mass transfer coefficient, m/s
K_a	equilibrium constant for SMA model
K_d	dissociation constant for Langmuir isotherm, mg/ml
n	value of valence of salt counterions
q	adsorbed protein density, mg/ml
q_m	adsorption capacity in Langmuir isotherm, mg/ml
q'	average solid-phase concentration at each collocation point, mg/ml
r	radial position in the particle, m
R	mean particle radius, m
$R_{e,p}$	$= u\rho d_p/(\mu\varepsilon_L)$, Reynolds number

S_c $= \mu/(\rho D_\infty)$, Schmidt number
t time, min
u liquid superficial velocity, cm/h
Z axial position in the column, cm
ε_L liquid-phase void fraction of expanded bed
ε_p effective intraparticle porosity for protein
ε_s solids fraction in expanded bed
ρ solution density, kg/m^3
μ solution viscosity, Pa·s
ν characteristic charge
σ_a protein steric factor

Acknowledgements

This work is supported by the Natural Science Foundation of China (Grant No. 20025617).

References

[1] R. Hjorth, Trends Biotechnol. 15 (1997) 230.
[2] F.B. Anspach, D. Curbelo, R. Hartmann, G. Garke, W.-D. Deckwer, J. Chromatogr. A 865 (1999) 129.
[3] P.R. Wright, B.J. Glasser, AIChE J. 47 (2001) 474.
[4] H. Zurek, E. Kubis, P. Keup, D. Hörlein, J. Beunink, J. Thömmes, M.R. Kula, C.P. Hollenberg, G. Gellissen, Proc. Biochem. 31 (1996) 679.
[5] Y.K. Chang, H.A. Chase, Biotechnol. Bioeng. 49 (1996) 204.
[6] J. Thömmes, M. Halfar, S. Lenz, M.R. Kula, Biotechnol. Bioeng. 45 (1995) 205.
[7] D. Lütkemeyer, N. Ameskamp, H. Tebbe, J. Wittler, J. Lehmann, Biotechnol. Bioeng. 65 (1999) 114.
[8] R.H. Clemmitt, H.A. Chase, Biotechnol. Bioeng. 67 (2000) 206.
[9] H.A. Chase, N.M. Draeger, Sep. Sci. Technol. 27 (1992) 2021.
[10] H.A. Chase, N.M. Draeger, J. Chromatogr. 597 (1992) 129.
[11] W.-D. Chen, X.-D. Tong, X.-Y. Dong, Y. Sun, Biotechnol. Prog. 19 (2003) 880.
[12] S. Veeraraghavan, L.T. Fan, A.P. Mathews, Chem. Eng. Sci. 44 (1989) 2333.
[13] C.A. Brooks, S.M. Cramer, AIChE J. 38 (1992) 1969.
[14] W.-D. Chen, Y. Sun, J. Chem. Ind. Eng. (China) 53 (2002) 88.
[15] W.-D. Chen, X.-Y. Dong, S. Bai, Y. Sun, Biochem. Eng. J. 14 (2003) 45.
[16] X.-D. Tong, Y. Sun, J. Chromatogr. A 943 (2002) 63.
[17] W.-D. Chen, X.-Y. Dong, Y. Sun, J. Chromatogr. A 962 (2002) 29.
[18] A.P. Van Der Meer, C.M.R.J.P. Blanchard, J.A. Wesselingh, Chem. Eng. Res. Des. 62 (1984) 214.
[19] L.S. Fan, Y.C. Yang, C.Y. Wen, AIChE J. 6 (1960) 482.
[20] J.H. Zhang, Q.A. Xu, Chemical Engineering Process Analysis and Computer Simulation, Chemical Industry Press, Beijing, 1989.
[21] Pharmacia Biotech, Q and S Sepharose Fast Flow-Product Data Sheet, Pharmacia Biotech, Uppsala, Sweden, 2002.
[22] J.F. Richardson, W.N. Zaki, Trans. Int. Chem. Eng. 32 (1954) 35.
[23] Y.K. Chang, H.A. Chase, Biotechnol. Bioeng. 49 (1996) 512.
[24] G. Dasari, I. Prince, M.T.W. Hern, J. Chromatogr. 631 (1993) 115.
[25] E. Pålsson, M.P. Nandakumar, B. Mattiasson, P.O. Larsson, Biotechnol. Lett. 22 (2000) 245.
[26] J. Thömmes, A. Bader, M. Halfar, A. Karau, M.R. Kula, J. Chromatogr. A 752 (1996) 111.
[27] H.B. Hu, S.J. Yao, D.Q. Lin, Z.Q. Zhu, Chin. J. Chem. Eng. 8 (2000) 230.
[28] S.R. Gallant, S. Vunnum, S.M. Cramer, J. Chromatogr. A 725 (1996) 295.
[29] L.J. Bruce, H.A. Chase, Chem. Eng. Sci. 56 (2001) 3149.